HHS Public Access

Author manuscript

Epilepsy Res. Author manuscript; available in PMC 2015 November 20.

Published in final edited form as:

Epilepsy Res. 2013 May ; 104(3): 253–263. doi:10.1016/j.eplepsyres.2012.10.015.

Cerebral reorganization after hemispherectomy: A DTI study

Avner Meoded[1], **Andreia V. Faria**[2], **Adam L. Hartman**[3], **George I. Jallo**[4], **Susumu Mori**[2,6], **Michael V. Johnston**[3,5], **Thierry A.G.M. Huisman**[1], and **Andrea Poretti**[1]

[1]Section of Pediatric Neuroradiology, Division of Pediatric Radiology, Russell H. Morgan Department of Radiology and Radiological Sciences, The Johns Hopkins University School of Medicine, Baltimore, MD, USA

[2]Russell H. Morgan Department of Radiology and Radiological Sciences, The Johns Hopkins University School of Medicine, Baltimore, MD, USA

[3]Department of Neurology, The Johns Hopkins University School of Medicine, Baltimore, MD, USA

[4]Department of Neurosurgery, The Johns Hopkins University School of Medicine, Baltimore, MD, USA

[5]Kennedy Krieger Institute, Baltimore, MD, USA

[6]F.M. Kirby Research Center for Functional Brain Imaging, Kennedy Krieger Institute, Baltimore, MD, USA

Abstract

Background and Purpose—To characterize changes in DTI scalars in WM tracts of the remaining hemisphere in children after hemispherectomy, assess the associations between WM DTI scalars and age at surgery and time since surgery, and evaluate the changes in GM fractional anisotropy (FA) values in patients compared to controls.

Materials and Methods—Patients with congenital or acquired neurological diseases who required hemispherectomy and high-quality postsurgical DTI data were included into this study. Atlas- and voxel-based analysis of DTI raw data of the remaining hemisphere was performed. FA, mean (MD), axial (AD) and radial (RD) diffusivity values were calculated for WM and GM regions. A linear regression model was used for correlation between DTI scalars and age at and time since surgery.

Results—19 patients after hemispherectomy and 21 controls were included. In patients, a decrease in FA and AD values and an increase in MD and RD values of WM regions were observed compared to controls ($p<0.05$, corrected for multiple comparisons). In patients with acquired pathologies, time since surgery had a significant positive correlation with white matter FA values. In all patients, an increase in cortical GM FA values was found compared to controls. ($p<0.05$)

Corresponding Author: Dr. Andrea Poretti, aporett1@jhmi.edu.

Conclusions—Changes in DTI metrics likely reflect Wallerian and/or transneuronal degeneration of the WM tracts within the remaining hemisphere. In patients with acquired pathologies, postsurgical FA values correlated positively with elapsed time since surgery suggesting a higher ability to recovery compared to patients with congenital pathologies leading to hemispherectomy.

Keywords

Hemispherectomy; Children; DTI; Neuroimaging; Neuroplasticity

Introduction

Hemispherectomy is a neurosurgical procedure to treat children with intractable seizures that start in childhood, arise diffusely from one hemisphere, and are associated with unihemispheric insults.[1,2] These include congenital (e.g. hemimegalencephaly and prenatal stroke) or postnatally acquired (e.g. Rasmussen encephalitis and traumatic brain injury) lesions.[1,3]

Postsurgical improvement of cognitive and behavioral functions is observed in children after hemispherectomy.[4–8] Motor, cognitive, and behavioral outcome after hemispherectomy, however, differ between children and depend on the etiology and time of onset of the underlying pathology and age of the child at neurosurgery.[6,9–11] These differences suggest that post-hemispherectomy plastic reorganization of brain circuitry may differ based on the underlying disease.

We used DTI to investigate the WM architecture of the remaining cerebral hemisphere in children after hemispherectomy. We 1) characterized the changes in DTI metrics in WM tracts of the remaining hemisphere in children after hemispherectomy and 2) assessed the associations between WM DTI scalars and a) age at and b) time since neurosurgery. We hypothesized 1) a secondary degeneration of WM tracts in patients compared to controls and 2) more severe changes in DTI scalars in patients with congenital compared to patients with postnatally acquired pathologies. Finally, we 3) evaluated the changes in GM fractional anisotropy (FA) values in patients compared to controls.

Materials and Methods

This retrospective study was approved by our institutional review board.

Subjects

The inclusion criteria for this study were 1) status post full anatomical hemispherectomy with sparing only of the basal ganglia and thalamus and 2) availability of post-surgical DTI data without artifacts. Demographic data and detailed information about etiology causing intractable seizures and leading to hemispherectomy (classified as *congenital* for cortical malformations and prenatally acquired lesions and *acquired* for postnatally acquired lesions), age at neurosurgery, and time interval between surgery and DTI study were collected by a review of the clinical charts.

Controls were selected from our neuroimaging database using three criteria: 1) normal brain anatomy, 2) absence of neurological disorders, and 3) availability of DTI raw data. MRI studies of the controls were acquired for clinical indications such as facial skin lesions or evaluation of soft tissue pathologies confined to the head and neck region.

DTI acquisition

DTI data were acquired on two 1.5 T scanners (Philips Medical Systems, Best, Netherlands; Siemens Avanto, Erlangen, Germany). On the Philips, DTI dataset was acquired with a multislice, single-shot echo-planar imaging (SENSE factor = 2.5) spin echo sequence. Diffusion weighting was applied along 32 directions with a b-value of 700 s/mm^2. Five minimally weighted images (b-value=33s/mm^2) were also acquired. For the acquisition of the DTI data, the following parameters were used: slice thickness=2.5mm, FOV=240×240mm, and matrix size=96×96, reconstructed/interpolated to a matrix of 256×256. The acquisition was repeated three times to enhance the SNR.

DTI parameters on Siemens scanner: 20 non-collinear directions and a high b-value of 1000s/mm^2 was used. An additional measurement without diffusion weighting (b=0s/mm^2) was performed. For the acquisition of the DTI data, the following parameters were used: slice thickness=2.5mm, FOV=240×240mm, and matrix size=192×192. Parallel imaging iPAT=2 with GRAPPA (generalized auto-calibrating partial parallel acquisition reconstruction) was used. The acquisition was repeated twice to enhance the SNR.

DTI post-processing

DTI post-processing was performed off-line using MRI Studio software (H. Jiang & S. Mori, Johns Hopkins University, available at www.MriStudio.org). The raw diffusion-weighted images were first co-registered to one of the least diffusion-weighted images and corrected for eddy current and subject motion. The following maps were generated: FA, color-coded FA, trace of diffusion, axial (AD) and radial (RD) diffusivity, and mean b0. After skull-stripping, the images were subsequently normalized to the MNI coordinates using b0 images for both the subject and the template. Two “half brain templates” including only one cerebral hemisphere (right and left, respectively) were previously created using the JHU-MNI template (Supplementary Figure 1). Subsequently, a transformation using a dual-contrast (FA and trace of diffusion) large deformation diffeomorphic metric mapping (LDDMM) was applied.

As the next step, atlas-based analysis (ABA) was performed using the WM parcellation map of the “half brain JHU-MNI template” to parcellate the brain into 88 anatomical regions including both GM and WM. Because of the reciprocal nature of both linear and non-linear transformation, the transformation results were used to warp the parcellation map to the original DTI data, thus automatically segmenting each brain into the 88 subregions. After exclusion of the extra-cerebral spaces by a trace of diffusion threshold at 0.0045, FA, mean diffusivity (MD), AD, and RD values were calculated for following categories of tracts 1) projection tracts: posterior limb of internal capsule (PLIC), anterior, superior, and posterior corona radiata, (ACR, SCR, PCR), 2) association tracts: cingulate bundle at the cortex (CGC), cingulate bundle-hippocampal part (CGH), superior longitudinal fasciculus (SLF),

and superior fronto-occipital fasciculus (SFO), and 3) commissural tracts: genu, body, and splenium of the corpus callosum (GCC, BCC, SCC) of the remaining hemisphere.[12] In addition, DTI metrics were collected for the following GM structures: superior parietal, frontal, temporal occipital, precentral, postcentral, and cingulate gyri as well as thalamus and putamen.

After ABA, voxel-based analysis (VBA) was performed by a normalization of the subject data to the template using the LDDMM matrix. Statistical parametric mapping was used to assess DTI scalars differences between all patients and controls. VBA was performed with SPM8 (www.fil.ion.ucl.ac.uk/spm/software/spm8) for Matlab version 2011b. After masking all images with the half brain template, and flipping all images to the left side, images were smoothed with a 10-mm full width at half maximum filter. The post-processed scans of the patient group were compared to the scans of controls using a two-sample *t* test, with scanner as covariate. For the statistical analysis, an explicit WM mask (FA threshold >0.2) created with ROI editor was used. VBA was performed for FA, MD, AD, and RD maps. In our analyses we used false discovery rate correction for multiple comparisons with $p<0.05$ and 30-voxel extent threshold. Finally, after controlling for correlation for right and left structures in our controls we flipped the right half brain to the left for all patients and controls, so analysis was done on the left hemisphere.

Statistical analysis

Statistical analyses were performed using SPSS Statistics version 21. Data obtained from ABA analysis was compared using a one-way ANCOVA with scanner type as a covariate. Post hoc analyses were performed using the Tukey's significant different test. To evaluate the associations between DTI scalars of the selected WM tracts and GM structures and 1) age at surgery and 2) time since surgery, a linear regression model was used in which age, gender, and disease duration, were considered as covariates. In all our analyses, observed differences were considered statistically significant if p-value was less than 0.05.

Results

Subjects

Nineteen patients (13 females, median age at MRI 12.2 years, range 0.9–25.0 years) and 21 controls (14 females, median age at MRI 12.2 years, range 0.9–29.0 years) were included in this study. Median age at surgery and median time since surgery were 3.8 years (range 0.8–12.9 years) and 7.2 years (range 0.02–18.0 years), respectively. Eleven (5 females) patients had a congenital etiology leading to hemispherectomy, 8 patients (all females) had an acquired etiology (Table 1). The median age at MRI for the patients with a congenital etiology was 8.9 years (range 0.9–20.5 years), median age at surgery 2.7 years (range 0.8–6.9 years), and median time since surgery 4.6 years (range 0.02–18.0 years). The median age at MRI for the patients with an acquired etiology was 14.9 years (range 3.9–25.0 years), median age at surgery 4.3 years (range 2.2–12.9 years), and median time since surgery 8.6 years (range 0.8–16.3 years).

Atlas-based analysis (ABA) of WM tracts

One-way ANOVA and post hoc analyses revealed significant changes in DTI scalars within projection (ACR, and PCR), association (CGC and SFO), and commissural (GCC, BCC, and SCC) tracts between patients after hemispherectomy and controls (Supplementary Tables 1 and 2). When significantly different, FA and AD values were lower and MD and RD values higher in patients after hemispherectomy compared to controls (Figure 1). DTI changes between both group of patients and controls involved commissural and association tracts more than projections tracts. A higher number of differences in DTI scalars and WM tracts was found between patients with congenital pathologies and controls compared to patients with acquired pathologies and controls. Between patients with congenital and acquired pathologies, only FA values in the CGC were significantly different and higher in the acquired group (Supplementary Figure 2).

Voxel-based analysis (VBA) of WM tracts

VBA showed decrease in FA as well as increase in MD and RD values in patients after hemispherectomy compared to controls (Figure 2). Changes in FA values were similar between VBA and ABA, while changes in MD and RD were more prominent for VBA compared to ABA. Compared to ABA, VBA did not reveal significant changes in AD. Changes in DTI scalars involved commissural and association tracts more than projections tracts confirming the ABA results.

Correlation between WM tracts DTI scalars and clinical parameters

In patients with acquired pathologies, age at surgery showed a significant negative correlation with FA values and a significant positive correlation with MD and RD values in projections tracts (Table 2). In the same group of patients, time since surgery had a significant positive correlation with FA values and a significant negative correlation with MD and RD values in projections fibers, cingulate bundle at the cortex, and genu of the corpus callosum. In patients with congenital etiology, however, only FA values within the cingulate bundle at the cortex showed a significant positive correlation with age at surgery and a significant negative correlation with time since surgery.

Atlas-based analysis (ABA) and correlation analysis of GM regions

ABA of cortical GM regions revealed significant reduction in FA values within the superior frontal, temporal, parietal, occipital, pre- and postcentral, and cingulate gyrus in all patients compared to controls (Figure 3). Within the putamen, however, FA values were significantly higher in the congenital group compared to both the acquired group and controls. MD, AD, and RD did not show significant differences between patients and controls; nor were statistically significant correlations with clinical measures observed.

Discussion

The ability of the central nervous system to adapt and reorganize following injury early in life is remarkable but has been difficult to study systematically in human infants. Data has been mostly accumulated from case studies and suggest that lesions sustained in early childhood are associated with better recovery.[13] This indicates a prominent structural

reorganization of the human brain.[14–16] The post-hemispherectomy brain offers a unique opportunity for studying the structural and functional neuroanatomical reorganization that underlies plasticity. Previous studies in patients after hemispherectomy applied DTI to study the reorganization of the motor and sensory tracts.[9,17,18] These studies showed marked trophic and microstructural changes within the ipsilesional corticospinal tract, while no differences were seen between the ipsi- and contralesional medial lemnisci.

We studied the contralateral (remaining) cerebral hemisphere using ABA and VBA.[19] These post-processing approaches are considered complementary.[20] ABA groups voxel values within a segmentation resulting in a marked reduction of information (from more than 1 million voxels within a brain to 176 anatomical regions). This reduction (voxel averaging) may lead to a higher statistical power, reduction of noise, and an easier biological interpretation. VBA, however, has a higher sensitivity to detect subtle abnormalities that may remain undetected by ABA. For both ABA and VBA, we used a half-brain template to avoid inaccurate normalization due to ipsilateral brain tissue remnants after anatomical hemispherectomy (e.g. thalamus). The accuracy of the brain parcellation hinges on the accuracy of the image transformation and subsequent atlas warping. Previous studies showed a high level of accuracy using the LDDMM algorithm for populations with marked anatomical distortions, various disease models, and different image conditions.[21,22] In our opinion, the use of a half-brain template and ABA as a low granularity filter helped to improve the parcellation accuracy in this study. Although state-of-art methods were used in all the steps, we cannot completely exclude minor inaccuracies within brain mapping.

In our study, ABA and VBA provided similar results including decrease in FA value and increase in MD and RD values in cerebral WM tracts of patients after hemispherectomy compared to controls. In addition, ABA revealed reduced AD values in cerebral WM tracts of patients compared to controls. Reduction in FA and AD associated with increase in MD and RD is suggestive of secondary Wallerian and/or transneuronal degeneration.[23] These changes in DTI scalars may indicate increase in isotropic tissue diffusion characteristics consistent with the presence of gliosis and the possible increase in extracellular matrix as shown by histology in Wallerian and/or transneuronal degeneration.

Between patients with congenital and acquired pathologies, the only significant difference was found in FA values of the CGC, which were lower in the congenital group. A previous fMRI study showed activation in the cingulate cortex after passive foot dorsiflexion in patients after hemispherectomy.[24] This may suggest a role of the CGC in rewiring cortical regions after hemispherectomy and assuming new functions such as motor tasks. Higher FA values suggest a better reorganization in the acquired group matching the better motor recovery in these patients.[10]

Highly different correlations were seen between both patients groups and age at surgery as well as time since surgery. In the acquired group, age at surgery negatively correlated with FA values, but had a positive correlation with MD and RD values in various components of the corona radiata. This suggests a more severe degeneration of projection fibers in children who were operated upon at an older age. In this group, early surgery may save the contralesional WM tracts from progressive degeneration and support/promote the greatest

postsurgical improvement with the application of rehabilitation techniques earlier during brain development.[25] Time since surgery, however, correlated well with an increasing (normalization) of FA values and reduction of MD and RD values in WM tracts. This correlation suggests that patients with an acquired pathology have a progressive neuronal reorganization.

For the congenital group we found less obvious results. Our structural findings match previous outcome studies that show a poorer post-hemispherectomy outcome in patients with congenital etiologies.[5,10] In patients with congenital pathologies structural and functional abnormalities have been shown within the “healthy” cerebral hemisphere.[26,27] Our findings are contrary to the Kennard principle suggesting that the immature brain should be more able to recover from injury than the more developed brain.[28] More recent studies showed that lesions occurring during critical phases of brain development may result in severe disabilities caused by disturbed development of the neuronal networks.

In cortical GM regions, ABA revealed a decrease in FA values in patients compared to controls. The reduction in anisotropy may reflect increased unoccupied intracellular space due to a change in neuronal cell density and/or reduction of the cortical neuropil. However, the significance of FA in GM is still poorly understood. Compared to WM, various cell types (e.g. neuronal cell bodies, randomly oriented axons, dendritic fibers, oligodendrocytes) and extracellular matrices are present in GM structures and may affect the diffusion properties and degree of anisotropy.[29,30] Putaminal FA values were significantly higher in the congenital group compared to both the acquired group and controls. This is an unexpected finding. Recently, increase in FA in GM structures after mild traumatic brain injury was shown to reflect progressive gliosis.[31] In this study, it is unclear whether increase in putaminal FA may reflect pre- or post-surgical gliosis in patients with congenital etiologies.

We are aware of some limitations of our study. Pre-hemispherectomy DTI data were not available for this study. Accordingly, we cannot exclude that presurgical WM microstructural alterations may partially explain postsurgical DTI changes. The number of patients is rather small. However, few previous pediatric studies are available due to the rarity of the surgical procedure. The two groups of patients are of different median age and have different age distributions. It is well known that with progressing brain maturation DTI scalars evolve. However, the most significant age-related changes in DTI scalars occur within the first 4 years of age.[32–34] Both studied groups of patients are significantly older (median ages of 8.9 and 14.9 years, respectively). The retrospective nature of this study made it impossible to correlate longitudinally collected clinical parameters of motor and cognitive functions and DTI scalars. Future prospective studies should include pre-surgical DTI data and longitudinally collected clinical parameters of neurological functions in order to evaluate neuroplasticity in children after anatomical hemispherectomy more accurately.

Conclusion

DTI is an ideal tool to study brain reorganization and may shed light on the structural cerebral plasticity in patients after hemispherectomy. Changes in DTI metrics reflect

Wallerian and/or transneuronal degeneration of the commissural, association, and projection WM tracts within the remaining hemisphere. In patients with acquired pathologies, postsurgical FA values tend to normalize over time suggesting a higher potential for recovery compared to patients with congenital etiologies leading to hemispherectomy.

Supplementary Material

Refer to Web version on PubMed Central for supplementary material.

Acknowledgments

Grant support:

Susumu Mori was funded by NIH grants: P41EB015909 and R01NS084957.

We are thankful to Amy Bastian, PhD, Kennedy Krieger Institute, Baltimore, MD, for sharing imaging data of some patients with us.

Abbreviation key

ABA	Atlas-based analysis
ACR	Anterior corona radiata
AD	Axial diffusivity
BCC	Body of the corpus callosum
CGC	cingulate bundle at the cortex
CGH	cingulate bundle-hippocampal part
CST	Corticospinal tract
FA	Fractional anisotropy
GCC	Genu of the corpus callosum
LDDMM	large deformation diffeomorphic metric mapping
MD	Mean diffusivity
PCR	Posterior corona radiata
PLIC	Posterior limb of internal capsule
RD	Radial diffusivity
SCC	Splenium of the corpus callosum
SCR	Superior corona radiata
SFO	superior fronto-occipital fasciculus
SLF	superior longitudinal fasciculus
VBA	Voxel-based analysis

References

1. Vining EP, Freeman JM, Pillas DJ, et al. Why would you remove half a brain? The outcome of 58 children after hemispherectomy-the Johns Hopkins experience: 1968 to 1996. Pediatrics. 1997; 100:163–71. [PubMed: 9240794]
2. Griessenauer CJ, Salam S, Hendrix P, et al. Hemispherectomy for treatment of refractory epilepsy in the pediatric age group: a systematic review. J Neurosurg Pediatr. 2015; 15:34–44. [PubMed: 25380174]
3. Kossoff EH, Vining EP, Pillas DJ, et al. Hemispherectomy for intractable unihemispheric epilepsy etiology vs outcome. Neurology. 2003; 61:887–90. [PubMed: 14557554]
4. Kossoff EH, Vining EP, Pyzik PL, et al. The postoperative course and management of 106 hemidecortications. Pediatr Neurosurg. 2002; 37:298–303. [PubMed: 12422044]
5. Jonas R, Nguyen S, Hu B, et al. Cerebral hemispherectomy: hospital course, seizure, developmental, language, and motor outcomes. Neurology. 2004; 62:1712–21. [PubMed: 15159467]
6. Pulsifer MB, Brandt J, Salorio CF, et al. The cognitive outcome of hemispherectomy in 71 children. Epilepsia. 2004; 45:243–54. [PubMed: 15009226]
7. Battaglia D, Chieffo D, Lettori D, et al. Cognitive assessment in epilepsy surgery of children. Childs Nerv Syst. 2006; 22:744–59. [PubMed: 16835686]
8. Devlin AM, Cross JH, Harkness W, et al. Clinical outcomes of hemispherectomy for epilepsy in childhood and adolescence. Brain. 2003; 126:556–66. [PubMed: 12566277]
9. Wakamoto H, Eluvathingal TJ, Makki M, et al. Diffusion tensor imaging of the corticospinal tract following cerebral hemispherectomy. J Child Neurol. 2006; 21:566–71. [PubMed: 16970845]
10. van der Kolk NM, Boshuisen K, van Empelen R, et al. Etiology-specific differences in motor function after hemispherectomy. Epilepsy Res. 2013; 103:221–30. [PubMed: 22974527]
11. Zhang J, Mei S, Liu Q, et al. fMRI and DTI assessment of patients undergoing radical epilepsy surgery. Epilepsy Res. 2013; 104:253–63. [PubMed: 23340329]
12. Wakana S, Jiang H, Nagae-Poetscher LM, et al. Fiber tract-based atlas of human white matter anatomy. Radiology. 2004; 230:77–87. [PubMed: 14645885]
13. Werth R. Visual functions without the occipital lobe or after cerebral hemispherectomy in infancy. Eur J Neurosci. 2006; 24:2932–44. [PubMed: 17156216]
14. Bittar RG, Ptito A, Reutens DC. Somatosensory representation in patients who have undergone hemispherectomy: a functional magnetic resonance imaging study. J Neurosurg. 2000; 92:45–51. [PubMed: 10616081]
15. Holloway V, Gadian DG, Vargha-Khadem F, et al. The reorganization of sensorimotor function in children after hemispherectomy. A functional MRI and somatosensory evoked potential study. Brain. 2000; 123(Pt 12):2432–44. [PubMed: 11099446]
16. Olausson H, Ha B, Duncan GH, et al. Cortical activation by tactile and painful stimuli in hemispherectomized patients. Brain. 2001; 124:916–27. [PubMed: 11335694]
17. Mori H, Aoki S, Abe O, et al. Diffusion property following functional hemispherectomy in hemimegalencephaly. Acta Radiol. 2004; 45:778–81. [PubMed: 15624522]
18. Choi JT, Vining EP, Mori S, et al. Sensorimotor function and sensorimotor tracts after hemispherectomy. Neuropsychologia. 2010; 48:1192–9. [PubMed: 20018199]
19. Oishi K, Faria AV, Yoshida S, et al. Quantitative evaluation of brain development using anatomical MRI and diffusion tensor imaging. Int J Dev Neurosci. 2013; 31:512–24. [PubMed: 23796902]
20. Faria AV, Zhang J, Oishi K, et al. Atlas-based analysis of neurodevelopment from infancy to adulthood using diffusion tensor imaging and applications for automated abnormality detection. Neuroimage. 2010; 52:415–28. [PubMed: 20420929]
21. Oishi K, Faria A, Jiang H, et al. Atlas-based whole brain white matter analysis using large deformation diffeomorphic metric mapping: application to normal elderly and Alzheimer's disease participants. Neuroimage. 2009; 46:486–99. [PubMed: 19385016]

22. Djamanakova A, Faria AV, Hsu J, et al. Diffeomorphic brain mapping based on T1-weighted images: improvement of registration accuracy by multichannel mapping. J Magn Reson Imaging. 2013; 37:76–84. [PubMed: 22972747]
23. Pierpaoli C, Barnett A, Pajevic S, et al. Water diffusion changes in Wallerian degeneration and their dependence on white matter architecture. Neuroimage. 2001; 13:1174–85. [PubMed: 11352623]
24. de Bode S, Firestine A, Mathern GW, et al. Residual motor control and cortical representations of function following hemispherectomy: effects of etiology. J Child Neurol. 2005; 20:64–75. [PubMed: 15791926]
25. Fritz SL, Rivers ED, Merlo AM, et al. Intensive mobility training postcerebral hemispherectomy: early surgery shows best functional improvements. Eur J Phys Rehabil Med. 2011; 47:569–77. [PubMed: 21508919]
26. Jahan R, Mischel PS, Curran JG, et al. Bilateral neuropathologic changes in a child with hemimegalencephaly. Pediatr Neurol. 1997; 17:344–9. [PubMed: 9436800]
27. Salamon N, Andres M, Chute DJ, et al. Contralateral hemimicrencephaly and clinical-pathological correlations in children with hemimegalencephaly. Brain. 2006; 129:352–65. [PubMed: 16291806]
28. Dennis M. Margaret Kennard (1899–1975): not a ‘principle’ of brain plasticity but a founding mother of developmental neuropsychology. Cortex. 2010; 46:1043–59. [PubMed: 20079891]
29. Komlosh ME, Horkay F, Freidlin RZ, et al. Detection of microscopic anisotropy in gray matter and in a novel tissue phantom using double Pulsed Gradient Spin Echo MR. J Magn Reson. 2007; 189:38–45. [PubMed: 17869147]
30. Yoshida S, Oishi K, Faria AV, et al. Diffusion tensor imaging of normal brain development. Pediatr Radiol. 2013; 43:15–27. [PubMed: 23288475]
31. Budde MD, Janes L, Gold E, et al. The contribution of gliosis to diffusion tensor anisotropy and tractography following traumatic brain injury: validation in the rat using Fourier analysis of stained tissue sections. Brain. 2011; 134:2248–60. [PubMed: 21764818]
32. Hermoye L, Saint-Martin C, Cosnard G, et al. Pediatric diffusion tensor imaging: normal database and observation of the white matter maturation in early childhood. Neuroimage. 2006; 29:493–504. [PubMed: 16194615]
33. Saksena S, Husain N, Malik GK, et al. Comparative evaluation of the cerebral and cerebellar white matter development in pediatric age group using quantitative diffusion tensor imaging. Cerebellum. 2008; 7:392–400. [PubMed: 18581196]
34. Cancelliere A, Mangano FT, Air EL, et al. DTI values in key white matter tracts from infancy through adolescence. AJNR Am J Neuroradiol. 2013; 34:1443–9. [PubMed: 23370472]

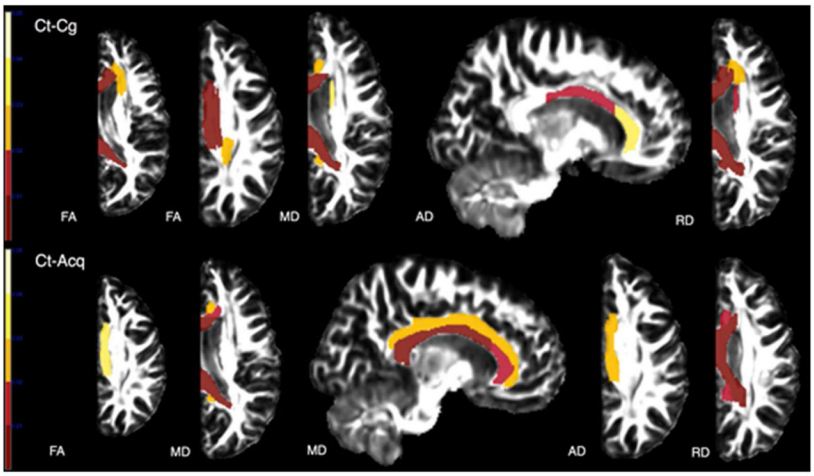

Figure 1.

Results of ABA. Compared to controls, patients with anatomical hemispherectomy because of a congenital and acquired underlying etiology showed decrease in FA and AD as well as increase in MD and RD in multiple WM tracts. Only results that survived the Tukey's significant different test are depicted with $p<0.05$. Color bars represent the p-values: 0.001–0.05 with color gradient from red to light yellow.

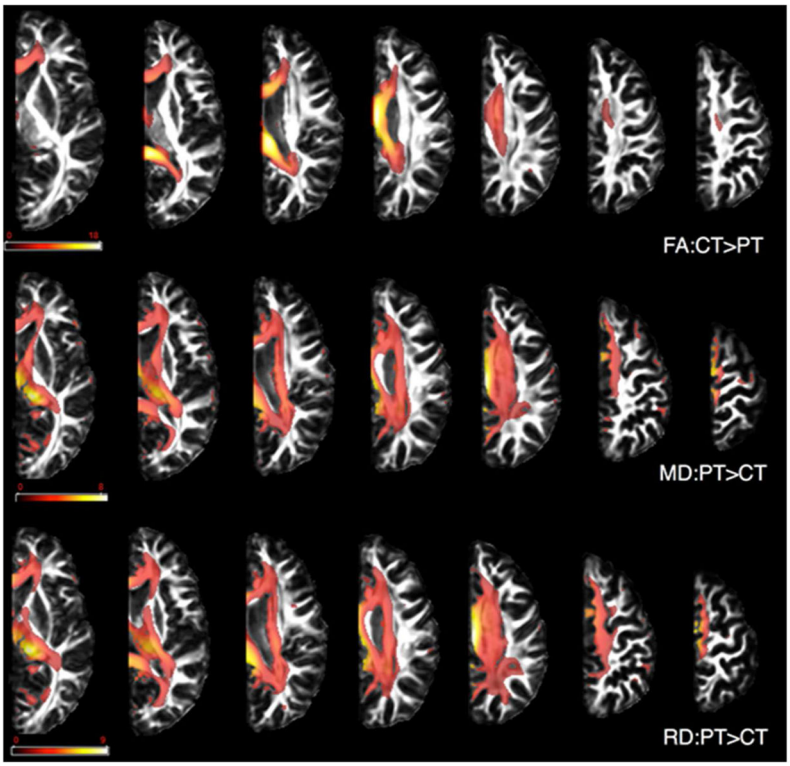

Figure 2.

Results of the VBA. Compared to controls, patients showed decrease in FA values and increased in MD and RD values in all examined WM tracts. Only results that survived false discovery rate correction for multiple comparisons are depicted with $p<0.05$. Color bars represent the T statistics.

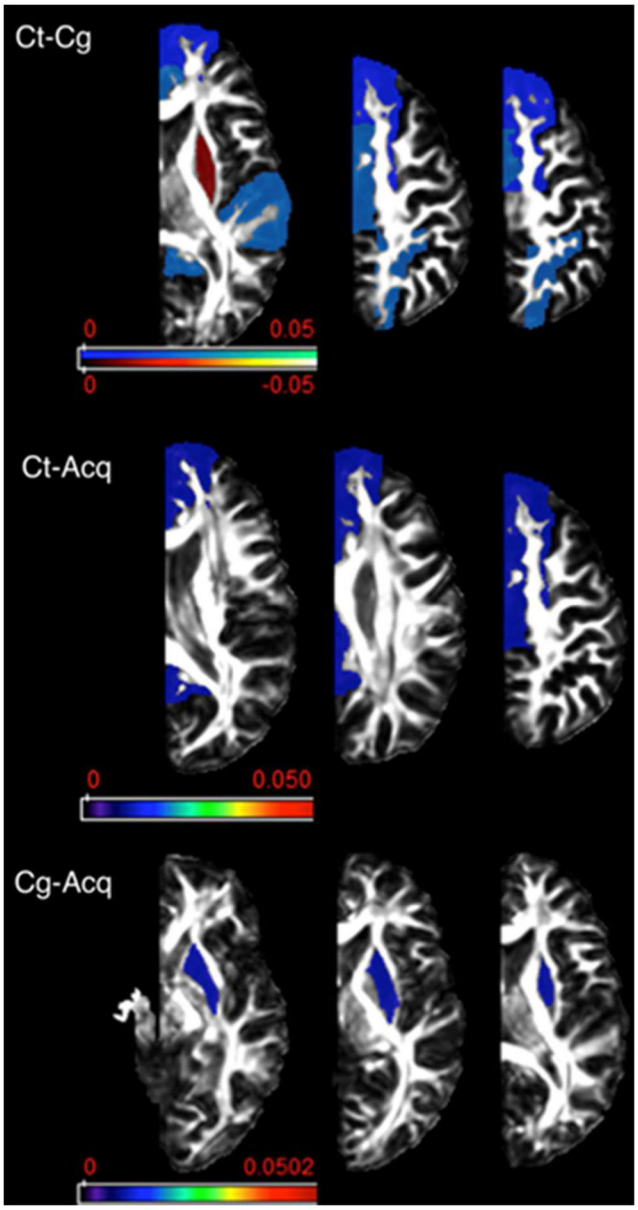

Figure 3.

Results of atlas-based analysis of GM structures. Compared to controls, patients in both etiology groups showed decreased FA in all the examined cortical areas with the exception of the putamen that showed increased FA in the congenital group. Only results that survived the Tukey's significant different test are depicted with $p<0.05$. Color bar represents the p-value: blue-light blue represent PT<CT and red-light yellow represent CT<PT.

Epilepsy Res. Author manuscript; available in PMC 2015 November 20.

Table 1

Demographic and clinical data of all patients with hemispherectomy

Patients	Gender	Age at study (years)	Age at surgery (years)	Time since surgery (years)	Diagnosis	Etiology group
1	M	8.1	5.9	2.2	HME left	congenital
2	M	3.3	1.1	2.2	HME left	congenital
3	M	14.8	3.7	11.1	Cortical dysplasia right*	congenital
4	M	2.2	0.9	1.3	HME left	congenital
5	F	2.7	2.7	0.02	Cortical dysplasia right*	congenital
6	M	12.9	5.7	7.2	Cortical dysplasia left*	congenital
7	F	11.5	6.9	4.6	Cortical dysplasia right*	congenital
8	F	0.9	0.8	0.1	HME left	congenital
9	M	14.0	2.3	11.7	Prenatal stroke right	congenital
10	F	8.9	4.1	4.8	Prenatal stroke left	congenital
11	F	20.5	2.5	18.0	Prenatal stroke right	congenital
12	F	8.7	2.2	6.5	Rasmussen right	acquired
13	F	3.9	3.1	0.8	Rasmussen left	acquired
14	F	18.1	9.8	8.3	Rasmussen right	acquired
15	F	15.2	3.8	11.4	Rasmussen right	acquired
16	F	12.2	4.1	8.1	Rasmussen right	acquired
17	F	25.0	12.9	12.1	Rasmussen right	acquired
18	F	20.7	4.4	16.3	Postnatal stroke right	acquired
19	F	14.5	5.7	8.8	Postnatal stroke right	acquired

F, female; HME, hemimegalencephaly; M, male;

*, includes an extensive unilateral malformation of cortical development affecting more than one cerebral lobe requiring full anatomical hemispherectomy rather than a more conservative neurosurgical approach.

Table 2

Significant correlations between DTI scalars in WM structures and clinical parameters in patients after hemispherectomy classified based on the underlying etiology

Clinical parameter	Etiology group	DTI scalars	WM tracts	Pearson correlation coefficient (r)	p-value	r square	adjusted r square
Age at surgery	Congenital	FA	CGC	0.840	0.001	0.71	0.67
	Acquired	FA	PLIC	−0.737	0.037	0.54	0.47
		RD	SCR	0.919	0.001	0.84	0.82
		MD	PCR	0.884	0.004	0.78	0.75
		RD	PCR	0.744	0.034	0.55	0.48
Time since surgery	Congenital	FA	CGC	−0.632	0.037	0.40	0.33
	Acquired	FA	PLIC	0.805	0.016	0.65	0.59
		RD	PLIC	−0.792	0.019	0.63	0.56
		RD	ACR	−0.802	0.017	0.64	0.58
		RD	SCR	−0.906	0.002	0.82	0.79
		MD	PCR	−0.788	0.020	0.62	0.56
		MD	CGC	−0.728	0.041	0.53	0.45
		FA	GCC	0.722	0.043	0.52	0.44

Pearson correlation coefficient, r square, adjusted r square, and p-value from multivariate linear regression analysis are shown.